Dielectric Properties of Mono- and Bilayers Determined from First Principles

Akash Laturia and William G. Vandenberghe
Dept. of Materials Science and Engineering
University of Texas Dallas
800 W. Campbell Rd., Richardson, TX-75080
Email: aal170030@utdallas.edu, wxv101020@utdallas.edu

***Abstract*—Two-dimensional materials, especially Transition Metal Dichalcogenide (TMDs), have emerged as a potential alternative to silicon for future electronic devices. We study the static out-of-plane dielectric constant for a range of single and bilayer two-dimensional materials. Dielectric response of these two-dimensional materials is studied using Density Functional Theory (DFT). Our calculations reveal that the dielectric constant increases with increasing chalcogen atomic number. The results also show that the ionic contribution to the dielectric response is much smaller compared to the electronic contribution.**

I. Introduction

With the exponential increase in research towards two-dimensional (2D) materials, a large focus lies in the study of their electronic and optical properties [1]–[4]. Optical and electrostatic properties of 2D materials are directly related to their dielectric response. In addition, the electronic and optical properties of mono-, bi- and few-layer 2D materials differ markedly as their band structure changes significantly with the number of layers. Thus we cannot expect bulk macroscopic dielectric constants to accurately describe dielectric behavior of mono-, bi- or few-layer materials.

For few-layer 2D materials such as graphene the dielectric properties are highly influenced by the surrounding medium [5]. Hence, one of the commonly adopted approach is to assign 2D materials the average dielectric constant of the surrounding media [6]. This approach is without justifcation however as it does not take into account the microscopic permittivity variations in the 2D material. Nevertheless, including microscopic permittivity variations is essential for an accurate solution of the Poisson equation $\nabla.[\epsilon(\mathrm{r})\nabla\phi_{\mathrm{tot}}(\mathrm{r})] = -\rho_{\mathrm{ext}}$; where $\epsilon(\mathrm{r})$ represents the spatial variation of dielectric permittivity.

We study the out-of-plane static dielectric constant of mono- and bilayer 2D materials. The macroscopic dielectric constant is computed from a microscopic permittivity. We consider a range of 2D materials, namely trigonal prismatic and octahedral transition-metal dichalcogenides (TMDs), as well as hexagonal boron nitride (h-BN).

II. Structural and Electrical Properties of 2D materials

A. Details of DFT calculations

We calculate the structural and electronic properties of mono- and bilayer 2D materials based on Density Functional Theory (DFT) calculations using a plane wave basis set and Projector Augmented Wave (PAW) pseudopotentials as implemented in the Vienna Ab Initio Simulation Package (VASP) [7]. The electron exchange correlation is treated in the generalized gradient approximation (GGA) as proposed by Perdew-Burke-Ernzerhof (PBE) [8]. Brillouin zone integrations are performed on a k-space grid of size $8 \times 8 \times 1$. The successive layers in a supercell are separated by a vacuum region of around $10a$ (a is in-plane lattice constant) to prevent any interaction between spurious replica images. All the bilayer structures are optimized until the variation in the total energy of the structure is less than 10^{-8} eV. The effect of transverse electric field is simulated using a sawtooth potential across the supercell while taking into account dipole corrections [9]. The value of the external field E_0 used for calculations is $\mp 0.01\ \frac{eV}{\AA}$ which is small enough to ensure that the 2D material operates in the linear response regime.

We consider both trigonal prismatic (H) and octahederally (T) coordinated 2D materials for dielectric analysis purposes. In a bilayer configuration the crystal structures with trigonal prismatic coordination tend to align in a staggered A-B stacking order. The two layers are shifted such that the chalcogens in the top (B) layer align with the metal in the bottom (A) layer. On the other hand octahedrally coordinated 2D materials tend to stack in an A-A' stacking order where the top (A') and bottom (A) layers are not shifted with respect to each other [10]. Monolayer h-BN is a planar 2D material with honeycomb lattice structure and it also follows an A-B stacking order in its bulk form. The structural parameters, namely the lattice constant (a) and the thickness (t) used for defining the monolayer 2D material structures are listed in Table I [11].

B. Out-of-plane dielectric constant

To study both the microscopic and macroscopic static out-of-plane dielectric constant we use the periodically repeated external potential as proposed by Resta and Kunc [12], [13]. As the thickness of the dielectric (t) is very small compared to the wavelength (λ) of the external applied potential, we can employ the long wavelength limit approximation to write the dielectric constant as the ratio of two macroscopic fields [14]. The combined dielectric response of the supercell, composed of the 2D material under study and the surrounding vacuum,

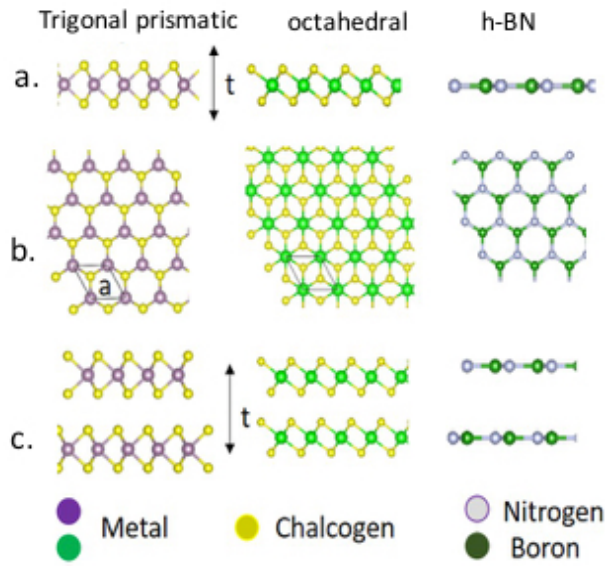

Fig. 1. (a) top view and (b) side view of mono layer trigonal prismatic (H), octahedrally (T) coordinated TMDs and h-BN respectively. Multilayer (H) coordinated TMDs stack in A-B configuration and T coordinated TMDs stack as A-A' configuration as illustrated in (c).

Material	a ()	t ()
MoS_2(H)	3.1604	6.25
$MoSe_2$(H)	3.288	6.53
$MoTe_2$(H)	3.517	7.00
WS_2(H)	3.154	6.181
WSe_2(H)	3.286	6.488
h-BN (H)	2.49	3.33
HfS_2(T)	3.635	5.837
$HfSe_2$(T)	3.748	6.159
ZrS_2(T)	3.662	5.813
$ZrSe_2$(T)	3.770	6.138

TABLE I
STRUCTURAL PARAMETERS USED IN OUR CALCULATIONS. a IS THE IN-PLANE LATTICE CONSTANT AND t IS THE THICKNESS OF THE MONOLAYER 2D MATERIAL.

is determined by the dielectric constant $\epsilon_{\rm SC}$ (where SC is a label referring to the supercell):

$$\epsilon_{\rm SC,\perp} = \frac{\rm E_0}{\rm E_{tot}} \tag{1}$$

$$\mathbf{E}_{\rm tot} = \mathbf{E}_0 + \mathbf{E}_{\rm induced} \tag{2}$$

where $\mathbf{E}_{\rm induced}$ is the induced electric field in the dielectric and $\mathbf{E}_0$ is the applied external field. The dielectric constant $\epsilon_{\rm sc}$ obtained from Eq. (1) represents the microscopic variations. $\mathbf{E}_{\rm tot}$ in Eq. (2) is obtained from

$$\mathbf{E}_{\rm tot}(\rm z) = -\partial_{\rm z} \rm V_{induced}(z) \tag{3}$$

where $\rm V_{induced}$ is the planar average of the difference in Hartree potential (obtained from DFT calculations) between finite electric field and zero electric field [15], [16]. Eventually the macroscopic dielectric constant is obtained by integrating the microscopic permittivity function using following equations:

$$\epsilon_{\rm sc}(\rm z) = \frac{\rm E_0}{\rm E_{tot}(z)} \tag{4}$$

and

$$\epsilon_{\rm SC} = \frac{1}{\rm c}\int_{\rm -c/2}^{\rm c/2} \frac{1}{\epsilon_{\rm SC}(\rm z)} \rm dz \tag{5}$$

Substituting Eq. (4) in Eq. (5) yields the following equation:

$$\epsilon_{\rm SC} = \frac{1}{\rm c}\int_{\rm -c/2}^{\rm c/2} \frac{\rm E_{tot}(z)}{\rm E_0} dz = \frac{1}{\rm c}\int_{\rm -c/2}^{\rm c/2} \frac{-\partial_{\rm z}\rm V_{induced}(z)}{\rm E_0} \rm dz$$

and finally

$$\epsilon_{\rm SC} = \frac{1}{\rm c}\frac{\rm V_{induced}(-c/2) - V_{induced}(c/2)}{\rm E_0}. \tag{6}$$

To illustrate the process of determining $\epsilon_{\rm SC}$, we show the induced charge density and the induced external potential in Fig. 2 for the case of monolayer $ZrSe_2$ and in Fig. 3 for the case of bilayer $ZrSe_2$. From the induced charge density plots for bilayer $ZrSe_2$ (Fig. 3) we see that most of the induced charge is concentrated around the individual layers.

C. Eliminating the contribution of vacuum to the dielectric response

The dielectric constant ($\epsilon_{\rm SC}$) computed in the previous section includes both a contribution of the 2D material and the vacuum. To obtain the dielectric constant corresponding to the 2D material we use the principle of equivalent capacitance and thereby eliminate the vacuum contribution:

$$\frac{1}{\epsilon_{\rm 2D}} = 1 + \frac{t}{c}\left(\frac{1}{\epsilon_{\rm SC}} - 1\right) \tag{7}$$

In Eq. (7) $\epsilon_{\rm 2D}$ is the relative permittivity corresponding to the 2D material, assumed to have thickness t. Inevitably, the value of $\epsilon_{\rm 2D}$ depends on the value of the thickness that is assumed. As a physically meaningful thickness value, we employ the interlayer distance in bilayer configurations, as computed by VASP when enabling ionic relaxation. In other words, t in Eq. (7) is the distance between successive layers of a bilayer 2D material. The values of thicknesses used for various materials are listed in Table I. Going back to our example illustrated in Figs. 2-3, the dielectric constant of mono- and bilayer $ZrSe_2$ are found to be 7.10 and 8.37 respectively.

The values of the out-of-plane dielectric constant for a larger set of 2D materials, computed using Eq. (7), are listed in Table II [17]. As can be seen in Fig. 4, hexagonal boron nitride (h-BN) has the smallest dielectric constant of all 2D materials with no difference between bilayer and monolayer values. For TMDs, dielectric constants are increasing with increasing chalcogen atomic number, i.e. $\epsilon_{\rm MTe_2} > \epsilon_{\rm MSe_2} > \epsilon_{\rm MS_2}$. Dielectric constants increase on average by 7.5% for all bilayers compared to their monolayer counterparts.

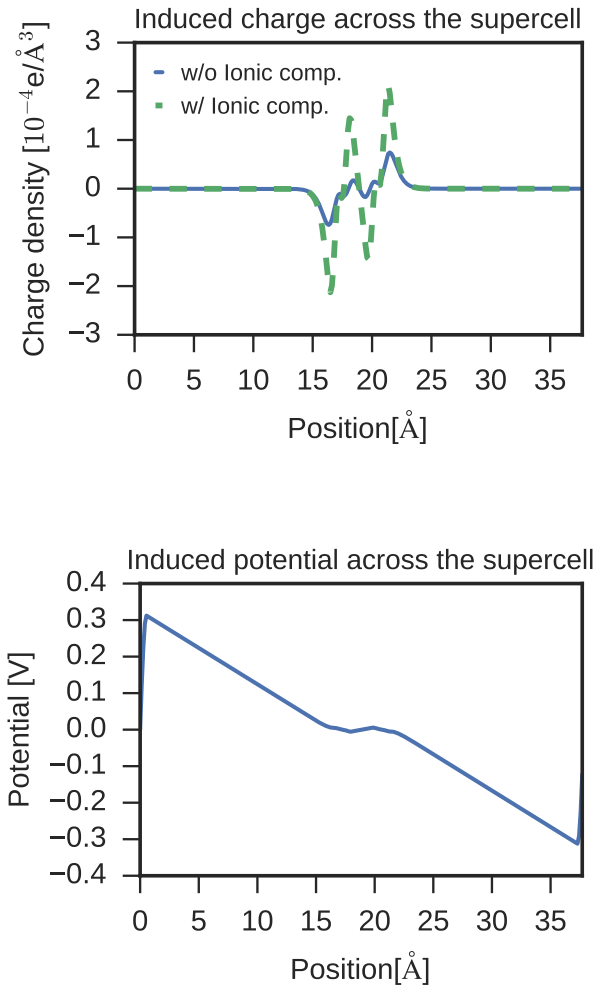

Fig. 2. Monolayer $ZrSe_2$: Induced charge (top) and induced potential (bottom) profile across the supercell.

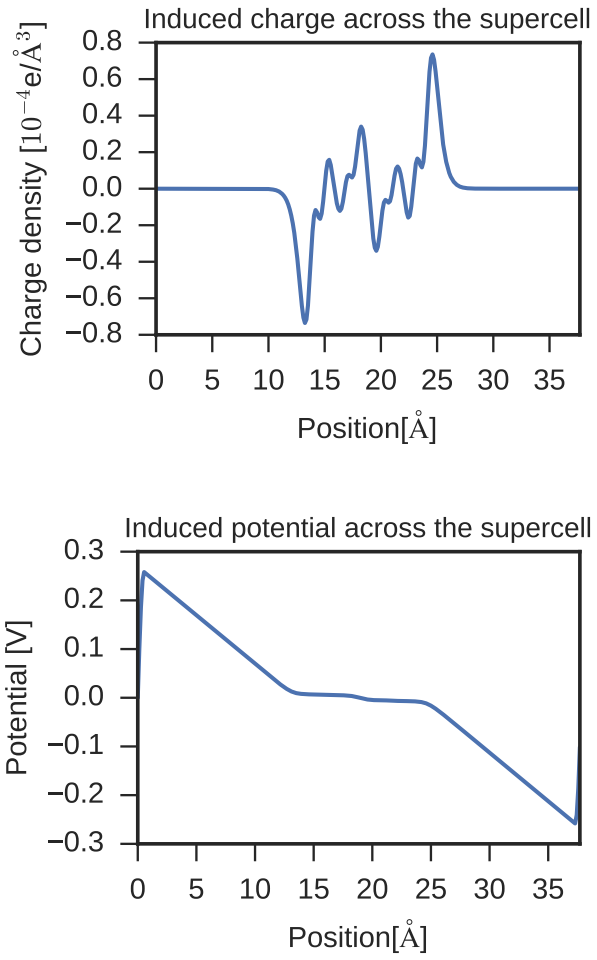

Fig. 3. Bilayer $ZrSe_2$: Induced charge (top) and potential profile (bottom) across the supercell.

III. Ionic Contribution To The Dielectric Response

The dielectric constant calculated in the previous section represents only the electronic contribution to the dielectric response as all the ions are frozen in the presence of the electric field. To compute the dielectric constant including its ionic component, we repeat the previous calculation permitting the ions to relax. The ionic contribution to the dielectric constant is computed only for monolayer 2D materials. During the relaxation, the in-plane lattice constant and the volume of the unit cell are kept intact but now allowing the ions to change their position in the presence of the external electric field. Fig. 2 shows the effect of an applied electric field on the induced charge distribution due to change in the position of ions for monolayer $ZrSe_2$. This change in induced charge density causes a change of $\approx 12\%$ in the macroscopic dielectric constant obtained for $ZrSe_2$.

The dielectric constant values including and excluding the ionic polarization (obtained from calculations) are listed in

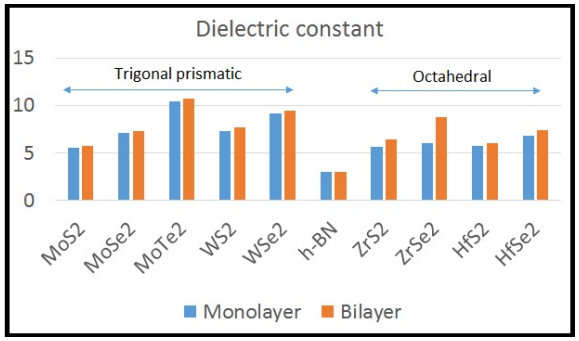

Fig. 4. Dielectric constant values of monolayer and bilayer 2D materials under study, as listed in Table II.

Table II. It can be seen from Fig. 5 that the electronic component dominates the overall dielectric response. Also no significant changes in the dielectric constants are observed for 2D materials with trigonal prismatic coordination when the ionic component is included. The ionic contribution is significant for octahedrally coordinated 2D materials as indicated by

Material	Monolayer ($\epsilon_{e,\perp}$)	Bilayer ($\epsilon_{e,\perp}$)	Monolayer ($\epsilon_{e+i,\perp}$)
MoS_2(H)	5.5	5.8	5.5
$MoSe_2$(H)	7.0	7.3	7.1
$MoTe_2$(H)	10.4	10.7	10.7
WS_2(H)	5.8	6	5.9
WSe_2(H)	7.4	7.8	7.4
h-BN	2.6	2.6	3.0
HfS_2(T)	5.0	5.2	5.9
$HfSe_2$(T)	6.5	6.8	7.3
ZrS_2(T)	5.4	5.7	6.3
$ZrSe_2$(T)	7.1	8.4	8.3

TABLE II
OUT-OF-PLANE DIELECTRIC CONSTANTS $\epsilon_{e,i,\perp}$ FOR MONO- AND BILAYER 2D MATERIALS . $\epsilon_{e,\perp}$ REPRESENTS THE ELECTRONIC CONTRIBUTION TO THE DIELECTRIC CONSTANT WHEREAS $\epsilon_{e+i,\perp}$REPRESENTS BOTH IONIC AND ELECTRONIC CONTRIBUTION TO THE OUT-OF-PLANE DIELECTRIC CONSTANT.

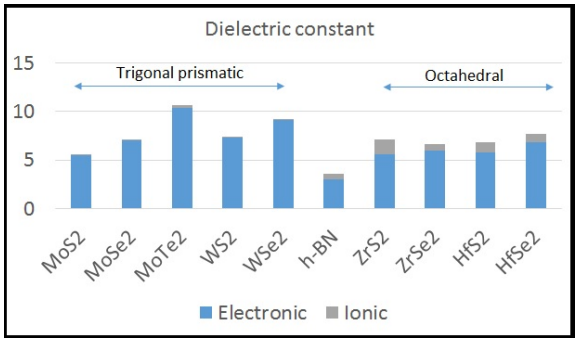

Fig. 5. Electronic and ionic contribution to dielectric response of mono layer 2D materials.

an average increase in dielectric constant values of about 18%. This relatively significant contribution of the ionic component to dielectric response for octahedral co-ordination as compared to trigonal prismatic co-ordination can be attributed to the absence of mirror symmetry in the former.

IV. Conclusion

We have calculated the static dielectric constant for several TMDs and h-BN in mono- and bilayer configurations from first principles calculations. We find that TMDs with higher atomic number chalcogens have higher dielectric constants. The dielectric constant increases by about 5% in bilayers for TMDs with trigonal prismatic coordination whereas the increase is about 10% for octahedral 2D materials with the exception of $ZrSe_2$ for which the increase is about 46%. Also for all the 2D materials under study, the electronic component dominates the overall dielectric response with the ionic contribution being much smaller.

Acknowlegment

We acknowledge the support of Nanoelectronics Research Initiative's (NRI's) Southwest Academy of Nano- electronics (SWAN). We would also like to thank Prof. M. Fischetti for insightful discussions.

References

[1] O. Lopez-Sanchez, D. Lembke, M. Kayci, A. Radenovic, and A. Kis, "Ultrasensitive photodetectors based on monolayer mos2," *Nature nanotechnology*, vol. 8, no. 7, pp. 497–501, 2013.

[2] M. V. Fischetti and W. G. Vandenberghe, "Mermin-wagner theorem, flexural modes, and degraded carrier mobility in two-dimensional crystals with broken horizontal mirror symmetry," *Physical Review B*, vol. 93, no. 15, p. 155413, 2016.

[3] A. S. Negreira, W. G. Vandenberghe, and M. V. Fischetti, "Ab initio study of the electronic properties and thermodynamic stability of supported and functionalized two-dimensional sn films," *Physical Review B*, vol. 91, no. 24, p. 245103, 2015.

[4] A. A. Balandin, S. Ghosh, W. Bao, I. Calizo, D. Teweldebrhan, F. Miao, and C. N. Lau, "Superior thermal conductivity of single-layer graphene," *Nano Letters*, vol. 8, no. 3, pp. 902–907, 2008, pMID: 18284217. [Online]. Available: http://dx.doi.org/10.1021/nl0731872

[5] M. V. Fischetti, W. G. Vandenberghe, B. Fu, S. Narayanan, J. Kim, Z.-Y. Ong, A. Suarez-Negreira, C. Sachs, and S. Aboud, "Physics of electronic transport in low-dimensionality materials for future fets," in *Simulation of Semiconductor Processes and Devices (SISPAD), 2014 International Conference on*. IEEE, 2014, pp. 1–4.

[6] E. J. Santos and E. Kaxiras, "Electrically driven tuning of the dielectric constant in mos2 layers," *ACS nano*, vol. 7, no. 12, pp. 10 741–10 746, 2013.

[7] P. E. Blöchl, "Projector augmented-wave method," *Phys. Rev. B*, vol. 50, pp. 17 953–17 979, Dec 1994. [Online]. Available: https://link.aps.org/doi/10.1103/PhysRevB.50.17953

[8] J. P. Perdew, K. Burke, and M. Ernzerhof, "Generalized gradient approximation made simple," *Phys. Rev. Lett.*, vol. 77, pp. 3865–3868, Oct 1996. [Online]. Available: https://link.aps.org/doi/10.1103/PhysRevLett.77.3865

[9] L. Bengtsson, "Dipole correction for surface supercell calculations," *Phys. Rev. B*, vol. 59, pp. 12 301–12 304, May 1999. [Online]. Available: https://link.aps.org/doi/10.1103/PhysRevB.59.12301

[10] R. J. Wu, M. L. Odlyzko, and K. A. Mkhoyan, "Determining the thickness of atomically thin mos 2 and ws 2 in the tem," *Ultramicroscopy*, vol. 147, pp. 8–20, 2014.

[11] J. Wilson and A. Yoffe, "The transition metal dichalcogenides discussion and interpretation of the observed optical, electrical and structural properties," *Advances in Physics*, vol. 18, no. 73, pp. 193–335, 1969. [Online]. Available: http://dx.doi.org/10.1080/00018736900101307

[12] K. Kunc and R. Resta, "External fields in the self-consistent theory of electronic states: A new method for direct evaluation of macroscopic and microscopic dielectric response," *Phys. Rev. Lett.*, vol. 51, pp. 686–689, Aug 1983. [Online]. Available: https://link.aps.org/doi/10.1103/PhysRevLett.51.686

[13] R. Resta and K. Kunc, "Self-consistent theory of electronic states and dielectric response in semiconductors," *Phys. Rev. B*, vol. 34, pp. 7146–7157, Nov 1986. [Online]. Available: https://link.aps.org/doi/10.1103/PhysRevB.34.7146

[14] L. Matthes, O. Pulci, and F. Bechstedt, "Influence of out-of-plane response on optical properties of two-dimensional materials: First principles approach," *Phys. Rev. B*, vol. 94, p. 205408, Nov 2016. [Online]. Available: https://link.aps.org/doi/10.1103/PhysRevB.94.205408

[15] J. Fang, W. G. Vandenberghe, and M. V. Fischetti, "Microscopic dielectric permittivities of graphene nanoribbons and graphene," *Phys. Rev. B*, vol. 94, p. 045318, Jul 2016. [Online]. Available: https://link.aps.org/doi/10.1103/PhysRevB.94.045318

[16] P. Kumar, B. S. Bhadoria, S. Kumar, S. Bhowmick, Y. S. Chauhan, and A. Agarwal, "Thickness and electric-field-dependent polarizability and dielectric constant in phosphorene," *Phys. Rev. B*, vol. 93, p. 195428, May 2016. [Online]. Available: https://link.aps.org/doi/10.1103/PhysRevB.93.195428

[17] B. Meyer and D. Vanderbilt, "Ab initio study of batio3 and pbtio3 surfaces in external electric fields," *Phys. Rev. B*, vol. 63, p. 205426, May 2001. [Online]. Available: https://link.aps.org/doi/10.1103/PhysRevB.63.205426